Research

Modelling Free-carrier Absorption in Solar Cells

Donald A. Clugston* and Paul A. Basore

Photovoltaics Special Research Centre, The University of New South Wales, Sydney 2052, Australia

Free-carrier absorption can be a significant parasitic optical absorption process in solar cells. Although estimates of its influence have been made in the past, it has not previously been incorporated into a numerical semiconductor device simulator and studied in conjunction with other effects. A finite element model of free-carrier absorption is presented that incorporates the dependency of the absorption coefficient on the carrier concentration profile, including the change in carrier density that occurs across a single finite element. This model has been implemented in the semiconductor modelling program PC1D for Windows, and used to simulate the effects of free-carrier absorption on several types of silicon solar cells. It was found to have only a very small effect on cell efficiency, but can significantly affect the long-wavelength spectral response, which has implications for device characterization. Empirical equations for the behaviour of free-carrier absorption in a variety of materials are presented. © 1997 John Wiley & Sons, Ltd.

INTRODUCTION

Free-carrier absorption is an optical absorption process that does not generate electron–hole pairs; instead, the photon energy is absorbed by free-carriers in either the conduction or valence band, moving the carrier to a higher energy state within that band. Free-carrier absorption has only a small impact on the total power output for most photovoltaic devices, but because it is heavily dependent on wavelength, it may still significantly affect the spectral response. This has implications for device characterization.

Despite some discrepancies in the reported behaviour of free-carrier absorption, sufficient data are available to construct a model that is adequate for solar cell simulation studies. Most published results[1–3] indicate that the free-carrier absorption coefficient depends linearly on the carrier concentration (at room temperature at least), although some studies[4,5] claim a dependence on the square-root of the carrier concentration for some materials. In view of this uncertainty, this paper uses the simpler assumption that the dependence is linear.

Free-carrier absorption is complex to implement in a numerical simulator because it depends on the carrier concentrations n and p, and is therefore: (i) not constant with time; (ii) not constant across a region of the device; and (iii) not constant across a single finite element.

* Correspondence to: D. A. Clugston, Photovoltaics Special Research Centre, University of New South Wales, Sydney 2052, Australia

PC1D for Windows[6] is a PC-based program that solves the semiconductor device equations in one dimension using a finite-element method. The previous photogeneration scheme used by PC1D was not sufficiently general to allow complex mechanisms such as free-carrier absorption to be included. Most importantly, it assumed that every absorbed photon generated an electron–hole pair. The aim of this work was to extend the scope of the photogeneration scheme used by PC1D.

THEORY

Consider a single element comprised of a thin layer of semiconductor material that is illuminated from one side by monochromatic light of wavelength λ and intensity T_0. Of this incident light:

(i)   a certain fraction G will generate electron–hole pairs;
(ii) a certain fraction L will be absorbed by parasitic processes and therefore lost;
(iii) the remainder T will be transmitted into the next element.

Optical absorption model used by previous releases of PC1D

Previous releases of PC1D assumed that $L = 0$. Thus, the transmission into the next element was simply $T = T_0(1 - G)$. Defining $T(x)$ as the photon flux at position x across the element, α_{eh} as the intrinsic absorption coefficient of the material and w as the width of the element, the relevant differential equation is simply

$$\frac{\mathrm{d}T}{\mathrm{d}x} = -\alpha_{eh} T(x) \tag{1}$$

with trivial solution

$$T(x) = T_0 e^{-\alpha_{eh} x}, \quad 0 \leqslant x \leqslant w \tag{2}$$

In this situation, $T = T(w)$, $G = T_0 - T(w)$.

Modelling of competing absorption processes

In the presence of free-carrier absorption, the differential equation ceases to be trivial. Without loss of generality, the following analysis assumes that the majority carriers are electrons, with distribution $n(x)$. The method used assumes that the absorption coefficient is of the form $\alpha_{FC} = f(\lambda)n(x)$, where f is some function of wavelength but is independent of position. Hence, the relevant differential equation is

$$\frac{\mathrm{d}T}{\mathrm{d}x} = -[f(\lambda)n(x) + \alpha_{eh}]T(x) \tag{3}$$

This equation is complicated by the fact that n is not necessarily constant across the element. Consequently, the photon flux does not simply decrease exponentially across the element; its behaviour is more complex. The calculated values for transmission and generation will depend on the assumed behaviour of n. The challenge is to find assumptions for the behaviour of n that are realistic yet manageable.

Assume that n varies exponentially across the element, from $n(0) = n_0$ to $n(w) = n_1$. Solution of the differential equation yields the intensity across the element, $T(x)$, as

$$T(x) = T_0 \exp\left(\frac{-wf(\lambda)n_0}{\ln(n_1/n_0)}\left[\left(\frac{n_1}{n_0}\right)^{(x/w)} - 1\right] - \alpha_{eh}x\right) \tag{4}$$

Although this expression has a complex dependence on x, the intensity of light remaining after passage through the element simplifies considerably

$$T = T_0 \exp\left(-\left[\frac{f(\lambda)(n_1 - n_0)}{\ln(n_1) - \ln(n_0)} + \alpha_{\text{eh}}\right]w\right) \tag{5}$$

This is one of the two results we need, as it gives the incident intensity for the subsequent element. It is a remarkably simple expression: it has a similar form to Equation (2), the transmission in the absence of parasitic processes. The total generation plus loss across the element is $G + L = T_0 - T$. But the determination of how much of this absorption is due to intrinsic absorption is more problematic.

The total absorption at point x across an infinitesimal slice of the element is $\alpha_{\text{eh}} + \alpha_{\text{FC}}$, so the fraction of the total absorption that generates electron–hole pairs is $\alpha_{\text{eh}}/(\alpha_{\text{eh}} + \alpha_{\text{FC}})$. The total generation across the element is thus

$$\int_0^w \frac{\alpha_{\text{eh}}}{\alpha_{\text{eh}} + \alpha_{\text{FC}}(x)} T_0[1 - e^{-\alpha_{\text{FC}}(x)x - \alpha_{\text{eh}}x}]\, dx \tag{6}$$

where

$$\alpha_{\text{FC}}(x) = \frac{wf(\lambda)n_0}{\ln(n_1/n_0)}\left[\left(\frac{n_1}{n_0}\right)^{(x/w)} - 1\right] \tag{7}$$

Unfortunately, this has no simple analytical solution. This leaves two alternatives: either evaluate the integral numerically, or make a further simplifying assumption. Equation (5) suggests such an approximation. Set

$$\alpha_{\text{FCeffective}} = f(\lambda)\frac{n_1 - n_0}{\ln(n_1) - \ln(n_0)} \tag{8}$$

Substitution of this expression into Equation (6) in place of α_{FC} gives the total generation as

$$G(x) = \alpha_{\text{eh}}/(\alpha_{\text{eh}} + \alpha_{\text{FCeffective}})[T_0 - T(x)] \tag{9}$$

Figure 1 illustrates the accuracy of Equation (9) in graphical form. Even with an unrealistically pessimistic situation (*n* varying by a factor of 10 across the element, large α_{eh} and $\alpha_{\text{FCeffective}}$), Equation (9) closely approximates the result obtained by numerically integrating Equation (6). However, Equation (9) ignores the spatial asymmetry of the finite elements. This is discussed further in the Appendix.

Validation of the approximate equation

Equation (9) was validated in two ways. Firstly, identical simulations were performed with different element sizes. This did not change the photogeneration. Secondly, Equation (6) was integrated numerically for a variety of pessimistic cases. It was found that Equation (9) was of an accuracy equivalent to at least a 10-point numerical integration. The errors introduced by Equation (9) were found to be smaller than round-off errors already present in PC1D. Equations (5) and (9) therefore form the basis of the free-carrier absorption model introduced in PC1D version 4.3.

The expression for $f(\lambda)$ was taken to be $A\lambda^B$, so that the final expression for α_{FC} is

$$\alpha_{\text{FC}} = An\lambda^B + Cp\lambda^D \ (\text{cm}^{-1}) \tag{10}$$

This is the expression for α_{FC} suggested by Chan.[7] Note that Equation (10) can be extended in complexity without invalidating Equation (9), provided that any additional terms are linearly dependent on the carrier concentrations.
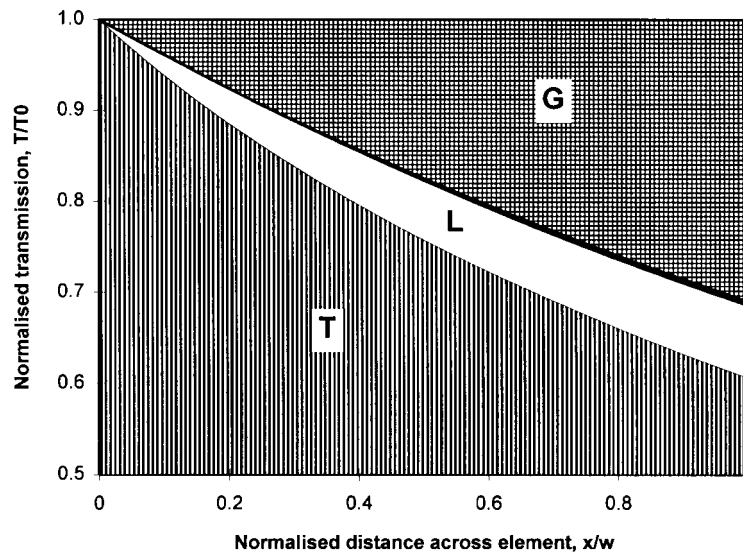
Figure 1. A graphical representation of the generation *G*, parasitic loss *L* and transmission *T* across a single finite element, assuming an exponential variation in carrier concentration across the element. The hatched areas were obtained by numerical integration of Equations (4) and (6). The thin black region illustrates the fraction of incident light that is incorrectly assigned to generation rather than loss by the 'effective α_{FC}' approximation in Equation (9)

MODELLING RESULTS AND DISCUSSION

A widely used empirical model for free-carrier absorption in silicon was presented by Schroder[1]

$$\alpha_{FC} = 1 \times 10^{-24} n\lambda^2 + 2.7 \times 10^{-24} p\lambda^2 \tag{11}$$

where α_{FC} is measured in cm^{-1}; *n* and *p* in cm^{-3} and λ in nm. This model is valid for large λ (> 5000 nm), but it ignores inter-conduction band excitation. For simulation of photovoltaic devices, only near-bandgap wavelengths are of interest. Examination of Schmid's data[3] shows that for this limited wavelength range, the absorption is better modelled by Green's model[9]

$$\alpha_{FC} = 2.6 \times 10^{-27} n\lambda^3 + 2.7 \times 10^{-24} p\lambda^2 \tag{12}$$

Several devices were simulated both with and without parasitic absorption, using this model.

Reduction in current density

Several commercial screen-printed cells with heavily doped *n*-type emitters were modelled. The relative reduction in short-circuit current induced by inclusion of free-carrier absorption is plotted against sheet resistance, for a variety of front diffusions (Figure 2). If the emitter sheet resistance is kept constant, increasing the doping does not greatly increase the free-carrier absorption losses, because the region of high doping is confined to a smaller volume. Typical cells will have an emitter sheet resistance of 30–50 $\Omega\ \square^{-1}$, constrained by the need for good blue response and good ohmic contact. From Figure 2, they will lose only $\sim 0.1\%$ of the current to free-carrier absorption.

These results are in general agreement with the calculations of Tiedje *et al.*,[8] which predict a theoretical maximum short-circuit current density of 41.1 mA cm^{-2} for an optimal solar cell. Tiedje predicts that 0.02 mA cm^{-2} would be lost due to free-carrier absorption, which corresponds to a relative loss of 0.05%. There are no corresponding constraints on doped regions at the rear of a cell. Very heavy doping
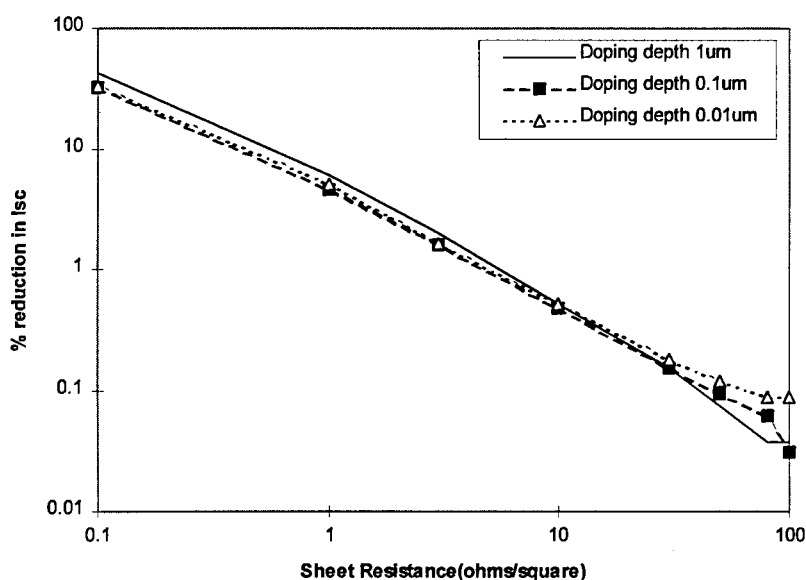
Figure 2. The reduction in I_{sc} due to free-carrier absorption for a screen-printed cell as a function of the sheet resistance of the emitter. Doping depths of 1, 0.1 and 0.01 μm are plotted. Error function diffusion profiles at the front of the device are assumed. These cells were $300 - μm$ thick single-junction devices with a base doping of 10^{16} cm^{-3}, and included front surface texturing, series resistance and shunt conductance

at the rear contact would cause the cell to suffer a large depreciation of current due to free-carrier absorption.

Green[9] has noted that free-carrier absorption may also be significant for cells attempting to boost the infrared response using novel techniques such as the impurity photovoltaic effect. Investigations by Keevers[10] indicate that free-carrier absorption is of primary importance in such techniques. Further work is required to quantify the effects of free-carrier absorption for each design.

It is clear that free-carrier absorption is not a major limiting factor in the efficiency of typical solar cells. Hence, neglect of free-carrier absorption does not invalidate calculations performed by previous releases of PC1D, except for a few exceptional cases.

Effect on internal quantum efficiency

Free-carrier absorption is strongly wavelength-dependent, and thus, although it does not greatly affect the efficiency of a device, it can change the shape of the cell's internal quantum efficiency (IQE) data, especially at long wavelengths. This can cause errors in subsequent analysis of the data if the analysis neglects parasitic absorption processes.

In the past, IQE data have been used to obtain a value for the internal optical reflection of the rear surface and to distinguish diffusion-length effects from rear-surface recombination. The method, developed by Basore,[11] uses a plot of IQE^{-1} versus α^{-1} (where α is the intrinsic absorption coefficient). The IQE measurements are performed for wavelengths up to 1120 nm, where the absorption is spatially uniform. However, this is the regime where free-carrier absorption begins to have an appreciable impact. This method has been further extended by Brendel *et al.*[12]

Neglect of free-carrier absorption will tend to underestimate the quality of the back-surface reflector and overestimate the electrical collection efficiency when Basore's method[11] is used. For a typical screen-printed cell, free-carrier absorption reduces the IQE at near-bandgap wavelengths by 2–3.5%. This causes an error of 4% in the calculation of rear-surface reflectance and electrical collection efficiency. The effect is stronger for more heavily doped cells. For example, the multilayer cell developed at the University of New

Table I. Free-carrier absorption coefficients for various semiconductors, for the model $\alpha_{FC} = nK\lambda^a$, where n is the carrier concentration (cm^{-3}) and λ is the incident wavelength (nm)

	K	a	Source
AlSb (n-type)	1.9×10^{-24}	2	Pankove[5]
GaAs (n-type)	4×10^{-29}	3	Pankove[5]
GaP (n-type)	(1.5×10^{-24})	(1.8)	Pankove[5]
GaSb (n-type)	9×10^{-31}	3.5	Pankove[5]
Ge (n-type)	$\sim 5 \times 10^{-25}$	~ 2	Pankove[5]
InAs (n-type)	6.5×10^{-29}	3	Pankove[5]
InP (n-type)	5×10^{-27}	2.5	Pankove[5]
InSb (n-type)	2.8×10^{-25}	2	Pankove[5]
Si (n-type)	2.6×10^{-27}	3	Green[9]
Si (p-type)	2.7×10^{-24}	2	Green[9]

South Wales[13] may have an IQE reduction of 13% at 1080 nm, leading to a 16–25% error in subsequent calculations. The validity of ignoring free-carrier absorption in the calculations can be determined approximately by measurement of the layer sheet resistance. Only cells with sheet resistance less than 50 $\Omega \ \square^{-1}$ are affected.

PARAMETERS FROM THE LITERATURE

Table I shows empirical estimates of the constants in Equation (10) obtained from the literature, for a variety of materials. Unfortunately, except for the data for silicon, all of these values were obtained by fits to long-wavelength data. The validity of these values for the region of interest to photovoltaic devices (near-bandgap range) has not been determined. More extensive theory[5,7] suggests that free-carrier absorption is made up of several mechanisms, each with a different dependency on λ. For acoustic phonons, the dependence is $\lambda^{1.5}$; for optical phonons it is $\lambda^{2.5}$; while for ionized impurities the dependence is λ^3 or $\lambda^{3.5}$. The total free-carrier absorption will be the weighted sum of these three processes; the dominant mode of scattering will depend on the impurity concentrations.[5] Hence, the exponent may increase slightly at high doping. This is confirmed by some experimental work, which indicates that the absorption coefficient is dependent on the chemical nature of the impurity, and also that (for Ge at least) α_{FC} becomes proportional to $n^{3/2}$ at high doping.[4,5] There are insufficient data, however, to justify a model more complex than Equation (10).

CONCLUSION

Free-carrier absorption is unlikely to reduce efficiency by more than about 0.5% for practical photovoltaic devices. However, because the effect is heavily dependent on wavelength, it may still significantly affect the spectral response. This has implications for device characterization. In particular, extended spectral analysis of a cell may underestimate the quality of the back-surface reflector and overestimate the electrical collection efficiency if free-carrier absorption is ignored in the calculations. The calculated values may differ from the correct values by over 20% in some cases. The validity of ignoring free-carrier absorption in the calculations can be determined approximately by measurement of the sheet resistance of the various layers in the cell. Only cells with sheet resistance less than about 50 $\Omega \ \square^{-1}$ are affected. Therefore, extended spectral analysis of a cell should be accompanied by measurement of the sheet resistance, to ensure that free-carrier absorption is not excessive.

The model used in this work has been incorporated into PC1D version 4.3, distributed by the University of New South Wales and released in October 1996. It can be used to quantify the effect of

free-carrier absorption on any situation of interest to the photovoltaic community. The e-mail address to obtain further information on PC1D is pc1d@unsw.edu.au.

APPENDIX: LIMITATIONS OF THE MODEL

Spatial asymmetry of the finite elements

The finite element model derived in this paper is spatially symmetric with regard to photogeneration. If one of the elements were flipped, the photogeneration profile would be unchanged. In reality, this result is not strictly correct because of the dependence on n and p, which are not usually symmetric across the element.

Interestingly, the transmission across the element is unaffected by such a spatial reflection. In physical terms, each photon must pass through every physical situation in the device, with an associated probability of capture. The total probability of capture is simply the product of all of the individual probabilities, and is therefore independent of the ordering of these physical situations. However, the probability of capture by a specific mechanism is heavily dependent on the ordering.

For example, consider the case where n is extremely high in an infinitesimal region of the element near one side, and low elsewhere. All of the free-carrier absorption therefore occurs at that single x value. Intrinsic absorption (producing electron–hole pairs) results in an exponential drop in intensity across the element. Figure 3 shows the intensity across an element for the two cases where all free-carrier absorption occurs either at the front (a) or at the rear (b) of the element. The vertical section of the curves (at $x = 0$ and $x = 1$, respectively) show the fraction of incident intensity lost to parasitic absorption. The generation across the element is different for the two cases, even though the transmission is identical.

In all physical situations of interest, however, spatial asymmetry is a very small effect. There are several factors that contribute to minimize its significance to PC1D. Firstly, it does not affect the value transmitted, so the errors will not compound across the device. Secondly, the error in Equation (9) reduces to 0 when $\alpha_{eh} \gg \alpha_{FC}$ or $\alpha_{FC} \gg \alpha_{eh}$, or when n_0 and n_1 are similar. Consequently, the error reduces as more elements are used. In PC1D, n_0 and n_1 never vary by more than a factor of two across an element. Thirdly, Equation (9) gives the average of the generation fractions for light entering from the front and rear of the element. The error reduces as light-trapping improves because a larger fraction of the light will traverse the element in both directions.
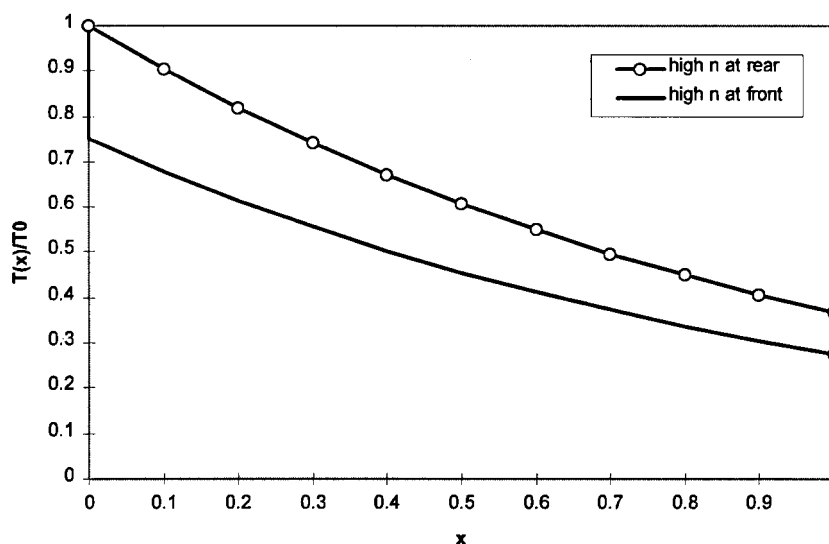

Figure 3. Spatial asymmetry of free-carrier absorption

Acknowledgements

REFERENCES

1. D. K. Schroder, R. N. Thomas and J. C. Swartz, 'Free carrier absorption in silicon', *IEEE Trans. Electron Devices*, **ED-25**, 254–261 (1978).
2. H. Y. Fan, W. Spitzer and R. J. Collins, 'Infrared absorption in n-type germanium', *Phys. Rev.*, **101**, 566–572 (1956).
3. P. E. Schmid, 'Optical absorption in heavily doped silicon', *Phys. Rev. B*, **23**, 5531 (1981).
4. S. C. Jain, A. Nathan, D. R. Briglio, D. J. Roulston, C. R. Selvakumar and T. Yang, 'Band-to-band and free-carrier absorption coefficients in heavily doped silicon at 4 K and at room temperature', *J. Appl. Phys.*, **69**, 3687–3690 (1991).
5. J. I. Pankove, *Optical Processes in Semiconductors*, pp. 75–76, Dover Publications, New York, 1971.
6. P. A. Basore and D. A. Clugston, 'PC1D for Windows: from analysis to design', *Proc. 25th IEEE Photovoltaic Specialists Conference*, May 1996, pp. 377–381.
7. B. O. Chan, 'Defects in silicon solar cell materials', *PhD Thesis*, pp. 25–32, University of New South Wales, Australia, 1993.
8. T. Tiedje, E. Yablonovitch, G. D. Cody and B. G. Brooks, 'Limiting efficiency of silicon solar cells', *IEEE Trans. Electron Devices*, **ED-31**, 711–716 (1984).
9. M. A. Green, *Silicon Solar Cells: Advanced Principles & Practice*, pp. 46–48, University of New South Wales, 1995.
10. M. J. Keevers and M. A. Green, 'Efficiency improvements of silicon solar cells by the impurity photovoltaic effect', *J. Appl. Phys.*, **75**, 4022 (1994).
11. P. A. Basore, 'Extended spectral analysis of internal quantum efficiency', *23rd IEEE Photovoltaic Specialists Conference*, May 1993, pp. 147–152.
12. R. Brendel, M. Hirsch, R. Pleininger and J. H. Werner, 'Experimental analysis of quantum efficiency for thin layer silicon solar cells with back surface fields and light trapping schemes', *Conf. Proc. 13th European Photovoltaic Solar Energy Conf.*, October 1995, pp. 432–435.
13. S. A. Edmiston, A. B. Sproul, M. A. Green and S. R. Wenham, 'Modelling of thin-film crystalline-silicon parallel multijunction solar cells', *Progr. Photovolt.*, **3**, 333–350 (1995).